

Comprehensive Assessment of Protein Conformational Stability and Unfolding Reversibility in Biotherapeutic Development via Intrinsic DSF and MSF

Overview

The development of biotherapeutics requires rigorous evaluation of both conformational and colloidal stability. In this application note, we introduce a new temperature cycling capability for the SUPR-DSF™ intrinsic differential scanning fluorimetry (DSF) platform, known in the literature as Modulated Scanning Fluorimetry (MSF). MSF enables direct assessment of protein folding reversibility, which correlates strongly with aggregation onset temperatures (T_{agg}) typically measured by Dynamic Light Scattering (DLS). Using representative protein systems, we demonstrate how MSF-derived insights complement traditional thermal stability (T_m) measurements. These results are obtained within a single experiment on the same instrument, while preserving the high throughput, low consumable cost, and minimal sample requirements of SUPR-DSF.

Introduction

The development of biotherapeutics requires rigorous assessment of protein stability, particularly with respect to conformational integrity. Thermal stability measurements provide direct insight into the folding landscape of a protein, enabling researchers to quantify unfolding transitions and compare the effects of formulation, mutations, or environmental conditions. Differential Scanning Fluorimetry (DSF) has become a widely adopted technique for this purpose due to its ability to monitor unfolding in real time with high sensitivity.^{1,2} Importantly, DSF leverages fluorescence to enable stability screening

across several orders of magnitude in protein concentration, offering highly comparable results but with greater flexibility than gold-standard techniques such as CD and DSC, which typically operate over narrower concentration windows.³

The SUPR-DSF platform builds on this foundation by leveraging intrinsic fluorescence detection to deliver high-quality thermal stability data in a high-throughput 384-well plate format, while minimizing sample consumption (10 μ L per well) and consumable cost (3 ϵ per sample).

While conformational stability is essential, it does not fully capture a protein's developability. Colloidal stability, particularly the propensity for stress-induced aggregation and loss of function (known as non-native protein aggregation), represents an equally important dimension of biophysical characterization.⁴ Dynamic Light Scattering (DLS) is commonly used to assess aggregation behavior and determine aggregation onset temperatures (T_{agg}). Some instrument platforms incorporate light scattering techniques alongside fluorescence-based measurements to address this need; however, this integration introduces important tradeoffs. Light scattering requires optically clear sample formats, such as quartz capillaries, which considerably increases consumable costs and limits compatibility with standard high-throughput plate formats. As a result, these approaches often sacrifice throughput and sample efficiency. In contrast, the SUPR-DSF platform is optimized for use with inexpensive, commercially available polypropylene qPCR plates, enabling higher-throughput, cost-effective analysis without these constraints.

For clarity, DSF in this application note refers to a standard intrinsic differential scanning fluorimetry experiment performed using a linear temperature ramp that results in a protein unfolding curve, whereas MSF refers to a temperature-cycling variant of intrinsic DSF that results in a nonreversibility curve. Both unfolding and nonreversibility curves can be obtained from an MSF experiment.

To bridge this gap, we introduce Modulated Scanning Fluorimetry (MSF), a new experiment type available only on the SUPR-DSF platform. MSF incorporates temperature cycling to directly assess the reversibility of protein unfolding, enabling determination of the non-reversibility onset temperature (T_{nr}). While T_{nr} and DLS-derived T_{agg} probe distinct phenomena, T_{nr} reflects the onset of irreversible processes that often precede or accompany aggregation, making it a correlated, practical proxy for colloidal stability.^{3,5,6} By delivering both conformational stability (T_m) and orthogonal aggregation-related insights (T_{nr}) within a single experiment on the same instrument, MSF expands the analytical capabilities of SUPR-DSF while preserving its core advantages of high throughput, low consumable cost, and minimal sample requirements.

SUPR-DSF: Advanced Protein Stability made Simple

SUPR-DSF (intrinsic Differential Scanning Fluorimetry) characterizes protein conformational stability using intrinsic fluorescence, enabling direct measurement of unfolding in the native state. During a thermal ramp, protein unfolding exposes buried hydrophobic residues, including tryptophan and tyrosine, producing measurable shifts in fluorescence intensity and emission wavelength. Unlike traditional dye-based DSF methods, which rely on extrinsic probes such as SYPRO Orange and may perturb protein stability or interact with formulation components, SUPR-DSF avoids added dyes entirely. This allows for analysis under native conditions and at high formulation concentrations without introducing assay artifacts.

A key advantage of the SUPR-DSF platform is its full-spectrum fluorescence acquisition, capturing emission data from 310–420 nm for every well. This enables flexible analysis of the fluorescence waveform using intensity, wavelength ratios, or barycentric mean (BCM), providing a more comprehensive view of unfolding behavior than single- or dual-wavelength approaches. The system supports high-throughput data collection in standard 384-well plates, resolving onset temperature (T_{onset}) and apparent melting temperatures (T_m) for complex multi-domain unfolding events. Using a proprietary autofitting algorithm, SUPR-DSF can deconvolute overlapping transitions and quantify independent domain stability with minimal user input. Data can be analyzed using thermodynamic (Boltzmann) fitting or a derivative-based approach utilizing Gaussian fitting of transition peaks. With the addition of MSF, the platform now enables determination of the non-reversibility temperature (T_{nr}), further extending its ability to characterize protein stability within a single, high-throughput experiment.

Modulated Scanning Fluorimetry: Assessing Unfolding Reversibility

While conventional linear thermal ramp experiments provide robust insight into thermodynamic transitions and endpoints, they offer more limited resolution into the kinetics, pathways, and reversibility of the unfolding process. While apparent T_m indicates the temperature at which half of the protein population is unfolded, it does not provide information regarding whether that unfolding step is reversible. In real-world manufacturing and storage scenarios, proteins are often exposed to transient thermal stress. If the unfolding is fully reversible, the protein returns to its functional native state once the stress is removed; however, if the unfolding is irreversible, partially or fully unfolded species may undergo irreversible processes, most notably aggregation, leading to loss of potency and increased developability risk.

MSF extends the conventional DSF experiment by incorporating incremental temperature cycling using the same hardware to directly assess refolding capacity. In this approach, described by Svilenov et al, the sample is heated to a defined target temperature, briefly incubated, and then cooled to a reference baseline where fluorescence recovery is measured.^{3,5,6} An example of this temperature cycling program and how it compares to a conventional linear DSF temperature ramp is illustrated in Figure 1. This cycle is repeated at incrementally higher temperatures, generating a nonreversibility profile that reflects the fraction of protein capable of returning to its native state as a function of exposure temperature. MSF experiments typically require 16–18 hours (i.e., overnight) for a single plate (up to 384 samples). This is comparable in length to high-quality DLS measurements with slow temperature ramps, but with a higher throughput.

During MSF experiments, proteins undergo multiple heating and cooling cycles, heating the samples up to a target temperature, then back down to a baseline temperature (Figure 1). Each time the protein reaches a new high temperature, and each time it returns to the baseline, its intrinsic fluorescence spectrum is measured.

As proteins fold and unfold, their fluorescence emission changes, so if their spectra at high temperatures has shifted compared to the baseline, we can surmise that an unfolding event has taken place. When the temperature returns to the baseline, if the spectrum returns to its original shape, then the unfolding is reversible.



However, if upon returning to the baseline temperature, the unfolded spectrum remains, we conclude that the unfolding was irreversible, resulting in permanent structural changes. This temperature at which unfolding becomes irreversible is called T_{nr} and fits next to T_m as a key indicator of protein stability.

The Nonreversibility Onset Temperature (T_{nr})

The primary parameter derived from MSF is the nonreversibility onset temperature (T_{nr}), defined as the temperature at which refolding efficiency begins to measurably decline. Operationally, T_{nr} is the temperature at which 10% of the protein shows non-reversible behaviour, as determined from a sigmoidal fit to the recovery-period fluorescence signal.⁵ This loss of reversibility is commonly driven by aggregation (although this change could also be driven by a permanent misfolding), where unfolded or partially unfolded species form irreversible intermolecular associations that outcompete refolding.

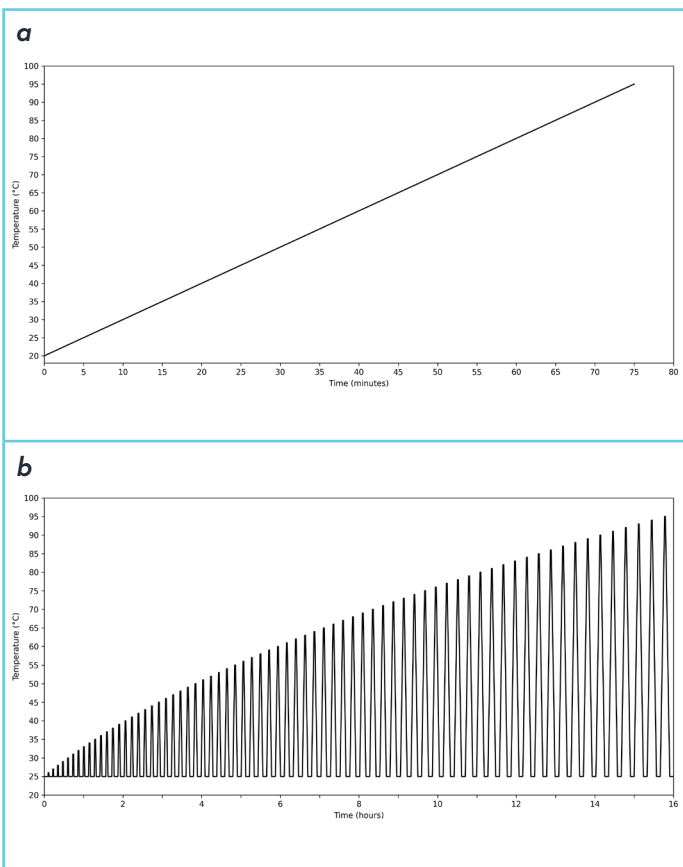


Figure 1: Plots of temperature (°C) versus time (minutes or hours). Example diagrams of a) a conventional linear DSF temperature ramp and b) an MSF temperature cycling program.

As a result, T_{nr} provides a practical indicator of a protein's susceptibility to aggregation under thermal stress. As mentioned above, the loss of reversibility can also be driven by permanent misfoldings and one major advantage of MSF is that the T_{nr} will take this into account, while T_{agg} determined by DLS will not.

Comparison to T_m

Both T_m and T_{nr} are measures of conformational stability; however, T_{nr} can differ significantly between proteins or formulations with similar T_m values, indicating that the two parameters do not necessarily correlate.⁵ While T_m represents the apparent unfolding temperature, it corresponds to the equilibrium midpoint of unfolding only when the process is fully reversible (i.e., when $T_{nr} \gg T_m$). In contrast, T_{nr} captures the onset of irreversible degradation pathways, such as aggregation or misfolding, making it particularly relevant for predicting long-term physical stability and formulation robustness.

Correlation Between Unfolding Reversibility (T_{nr}) and Aggregation Onset (T_{agg})

The importance of thermal unfolding reversibility as a determinant of aggregation resistance in antibody domains has been well established.⁷⁻¹¹ A key advancement in the application of MSF has been its ability to relate the nonreversibility onset temperature (T_{nr}) to the aggregation onset temperature (T_{agg}), typically measured by DLS. DLS is a powerful but lower-throughput, orthogonal technique that monitors increases in particle size (hydrodynamic radius; R_h) as proteins aggregate. While DLS directly measures the physical size of aggregates, MSF probes a common structural precursor to aggregation—the point at which a protein can no longer refold to its native state, leaving hydrophobic regions exposed and susceptible to intermolecular association.

Svilenov et al. investigated the relationship between DSF/MSF-derived parameters and DLS measurements across a panel of 13 therapeutic antibodies.⁶ On the one hand, they observed weak correlations between T_{nr} and T_{m1} ($R = 0.20$) and between T_{nr} and T_{onset} ($R = 0.46$), indicating that proteins can tolerate a degree of reversible unfolding before becoming irreversibly destabilized. A stronger correlation was found between T_{nr} and T_{m2} ($R = 0.75$), typically associated with Fab domain unfolding which tends to occur at more elevated temperatures.



On the other hand, an exceptionally strong correlation ($R = 0.93$) was observed between T_{nr} and T_{agg} . This finding suggests that, at least for the antibodies studied, aggregation as measured by DLS/ T_{agg} is the reason for the observed onset of nonreversibility by MSF/ T_{nr} . By demonstrating this relationship, MSF provides a high-throughput proxy for aggregation resistance, enabling efficient candidate ranking and formulation optimization using a single plate-based experiment.

Predictive Power for Storage Stability

The utility of T_{nr} extends beyond the laboratory bench to the prediction of long-term storage stability. In the stability study discussed above involving 13 monoclonal antibodies, forced degradation experiments demonstrated that those with higher T_{nr} values (typically above 75°C) were significantly more resistant to aggregation during storage at 40°C over several months. In contrast, antibodies with lower T_{nr} values showed a marked increase in the relative area of aggregates as measured by Size-Exclusion Chromatography (SEC). This evidence reinforces the role of T_{nr} as a pivotal developability metric, allowing for the early identification of "well-behaved" molecules that are likely to maintain high monomer content throughout their shelf life.

Results & Discussion

Analysis of three biomolecules via conventional DSF, MSF, and DLS

In this study, three proteins—anti-mouse IgG, human IgG, and HuCAL Fab—were analyzed in both a standard 75 minute DSF experiment, as well as an overnight MSF experiment using two identically prepared 384-well plates on the SUPR-DSF. Spectral data were processed to calculate the Barycentric Mean (BCM) of the fluorescence emission from 310–390 nm (fluorescence signal >390 nm is typically quite low for proteins). The intrinsic DSF experiment yielded T_{onset} and T_m values, while the MSF experiment provided T_{nr} in addition to T_{onset} and T_m , through analysis of BCM data at defined points during the temperature cycles. For T_{onset} and T_m values derived from the MSF experiment, BCM values were calculated from spectra acquired during the peak incubation periods, where the protein state most closely reflects that observed in a linear ramp. First-derivative BCM (dBCM) plots were then generated, and the resulting peaks corresponding to inflection points were fitted with Gaussian functions to quantitatively determine melting transitions under both experimental conditions. The dBCM plots are shown in Figure 2, and the corresponding T_{onset} and T_m values for the three proteins are summarized in Table 1.

All three constructs exhibit a T_{m1} in the range of approximately 70–72°C. The anti-mouse IgG shows a single apparent transition, the human IgG displays two resolvable transitions, and the HuCAL Fab presents a single transition, as expected. Both sets of values are in close agreement, with all T_m values within 1°C between experiments. This demonstrates that MSF, despite its longer overnight run time, produces melting temperatures comparable to DSF while also providing additional insight into protein nonreversibility.

To determine MSF-derived T_{nr} values, BCM data were calculated from spectra collected during the 25°C recovery periods at the troughs between cycle peaks, where the protein is expected to return to its initial folded state. BCM plots were generated and fitted with sigmoidal fits (Figure 3). T_{nr} values (vertical blue lines) were calculated using the same approach as T_{onset} values from unfolding datasets, with T_{onset} defined as the point at which the fitted curve deviates by 1% from the baseline (lower bound), while T_{nr} corresponds to a 10% deviation.

For reference, the vertical red line indicates the inflection point of the function, which can be interpreted as the midpoint (50%) of the nonreversibility transition. The gray data points in the background represent the corresponding BCM melt curve data derived from the cycle peaks. Of note, MSF can be applied to multidomain proteins to identify which unfolding transition drives nonreversibility. In Figure 3b, T_{nr} clearly coincides with the first unfolding transition, likely corresponding to the CH2 domain.¹²

Comparing T_{nr} (MSF) to T_{agg} (DLS)

Figure 4 compares the T_{onset} (onset of unfolding derived from the MSF dataset; defined as 1% unfolding), T_{nr} (MSF dataset; defined as 10% irreversible unfolding), and T_{agg} (DLS dataset; defined as a doubling of the observed particle radius) values for the three proteins. In an idealized case, one might expect the relationship $T_{onset} \leq T_{nr} \leq T_{agg}$ if conformational instability always precedes colloidal instability. From a conformational stability perspective, a protein must first begin to unfold (T_{onset}) before crossing the threshold (T_{nr}) where refolding is no longer the thermodynamically favored pathway and misfolding or aggregation result. For proteins that are colloidally stable under the conditions tested, T_{agg} would be expected to coincide with or occur after T_{nr} , reflecting the onset of aggregation and particle formation following irreversible structural changes. In practice, however, conformational and colloidal stability represent distinct biophysical properties, and real-world datasets often deviate from the simplified model.



Table 1: Comparison of T_{onset} and T_m values derived from DSF and MSF experiments. All values are calculated using Gaussian fits of the corresponding derivative (dBCM) curves from 310-390 nm and are an average of three replicate wells.

Experiment	DSF experiment (75 minutes) - provides T_{onset} & T_m		MSF experiment (18 hours) - provides T_{onset} , T_{m1} & T_{m2}	
Protein Construct	T_{onset} (°C)	T_m (°C)	T_{onset} (°C)	T_m (°C)
Anti-mouse (IgG)	63.23 ± 0.04	71.78 ± 0.07	60.79 ± 0.08	70.78 ± 0.03
Human IgG	61.16 ± 0.06	69.94 ± 0.07 (T_{m1}) 81.86 ± 0.30 (T_{m2})	59.30 ± 0.06	68.94 ± 0.02 (T_{m1}) 81.17 ± 0.09 (T_{m2})
HuCAL (Fab)	62.88 ± 0.09	72.43 ± 0.04	63.76 ± 0.17	72.20 ± 0.04

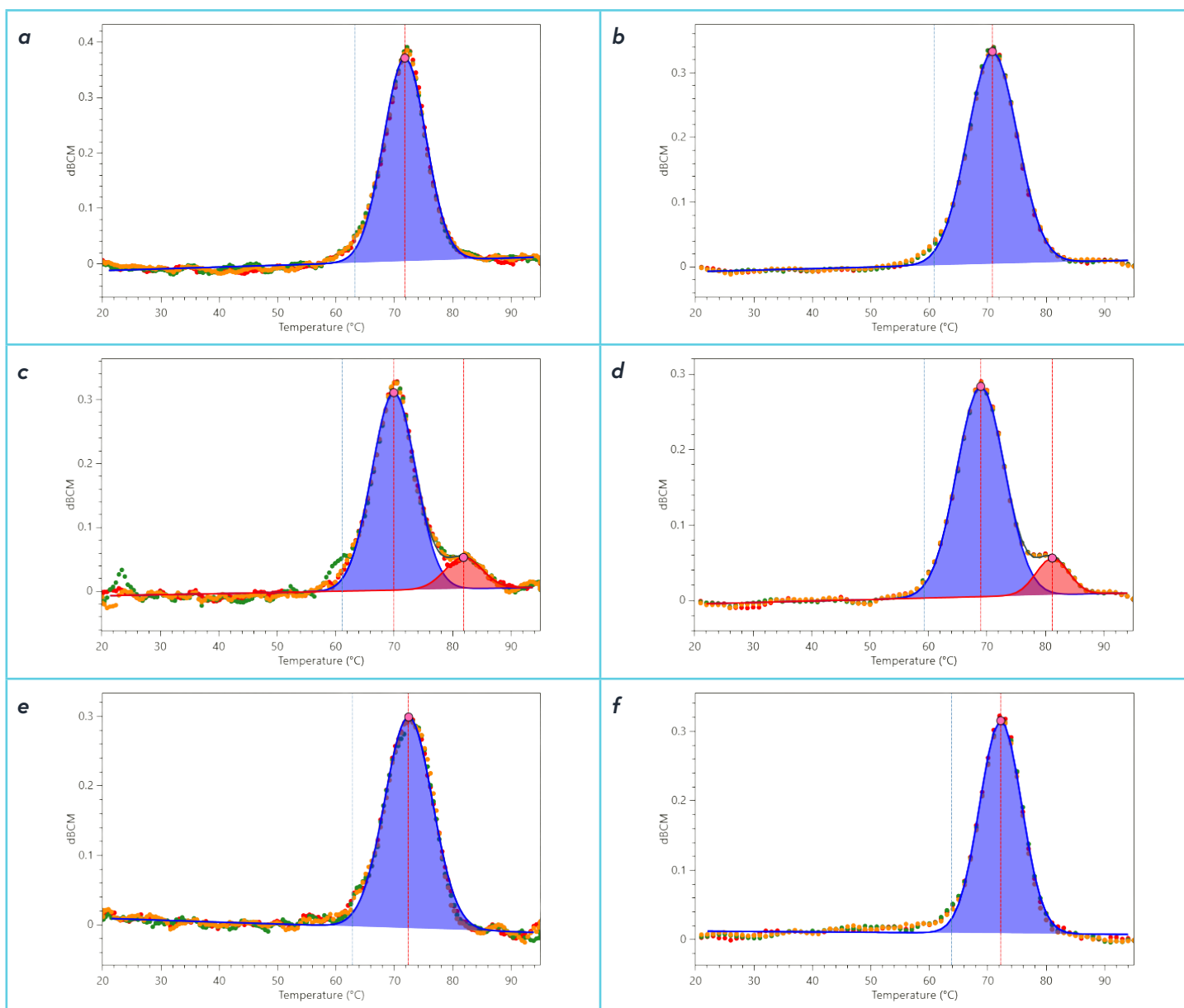


Figure 2: Comparison of overlaid triplicate dBCM thermal denaturation profiles obtained from a conventional DSF experiment (a, c, e) and an MSF experiment (b, d, f) for anti-mouse IgG (a & b), human IgG (c & d), and HuCAL proteins (e & f). The blue line represents T_{onset} and the red line represents T_m . The blue and red shaded areas represent the temperature regions of unfolding transitions corresponding to melting temperatures T_{m1} and T_{m2} , respectively.



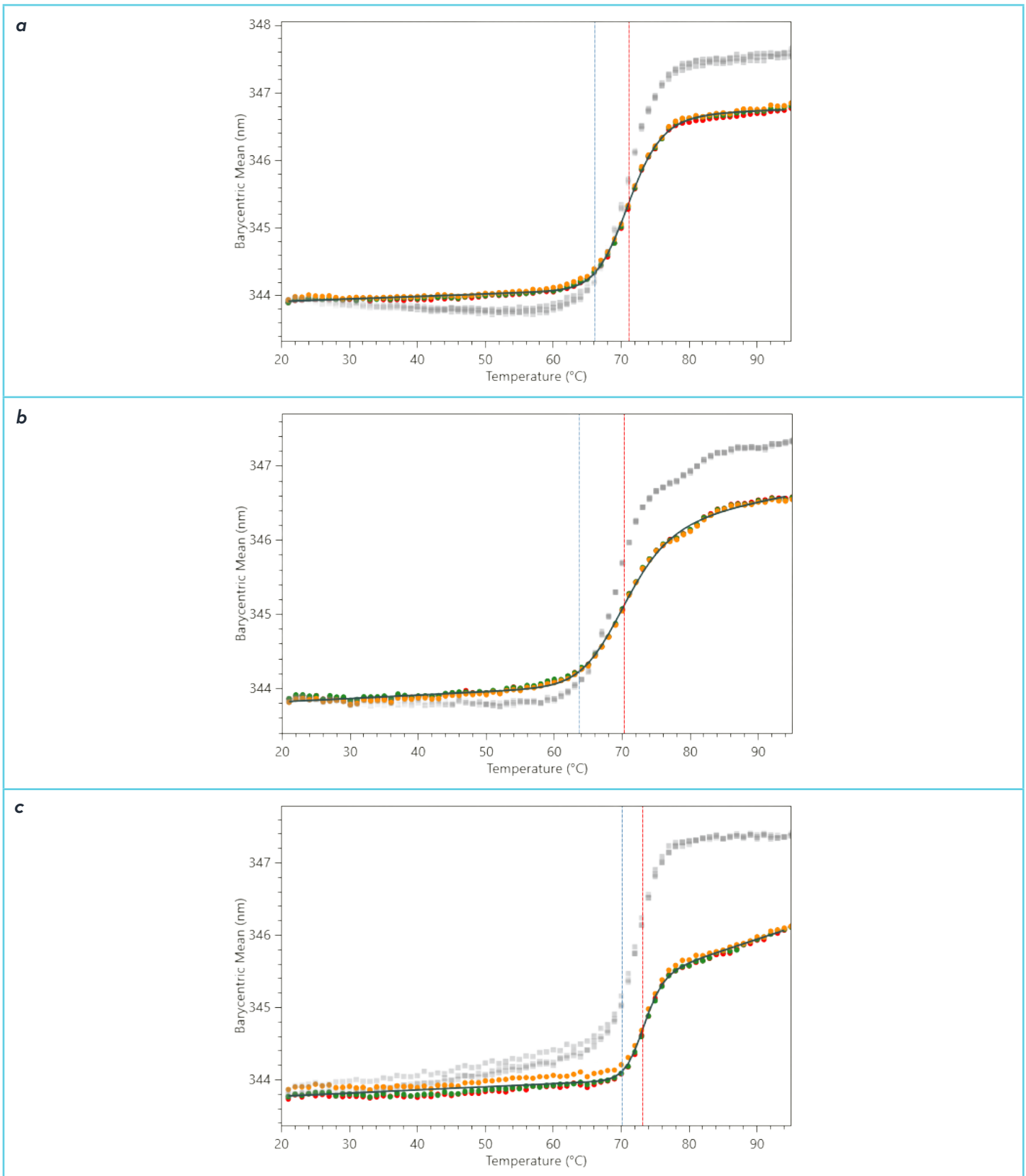


Figure 3: MSF plots for anti-mouse IgG (a), human IgG (b), and HuCAL (c). Data are shown in triplicate as BCM versus temperature. Colored data points (red, yellow, green) with blue sigmoidal fit curves represent the MSF data, while gray data points correspond to the BCM melt curve data derived from the cycle peaks. The vertical blue line indicates T_{mr} , defined as the point at which the fitted curve deviates by 10% from the sigmoid baseline (lower bound). For reference, the vertical red line marks the inflection point of the



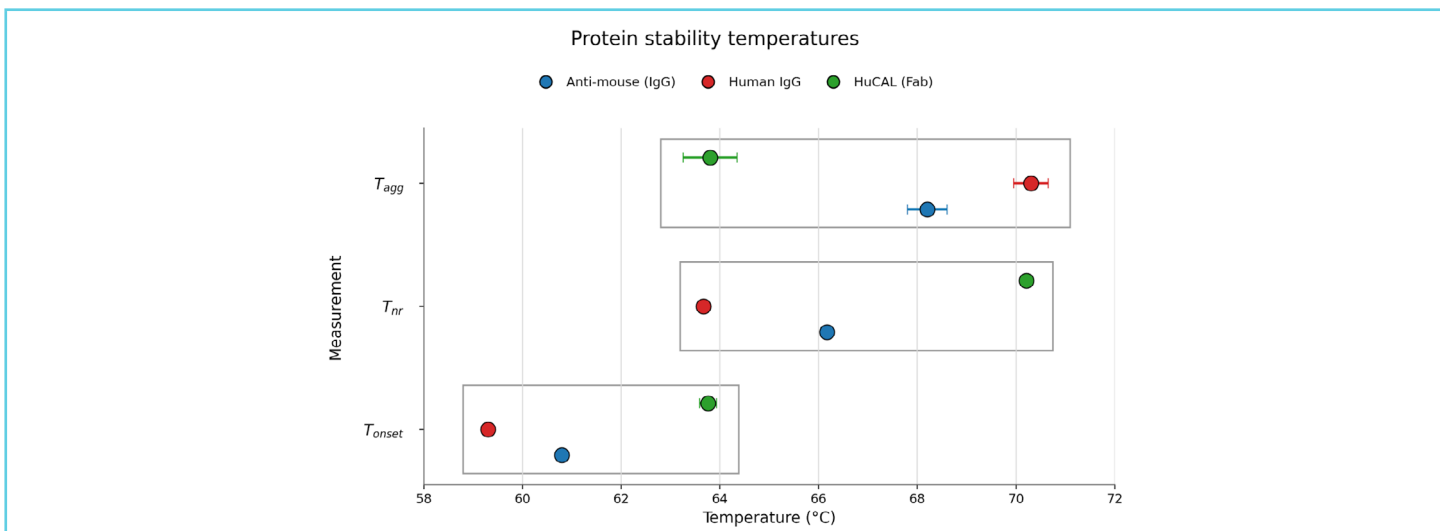


Figure 4: MSF-derived T_{nr} values were obtained from sigmoidal fits of BCM data (310–390 nm) using a 10% deviation threshold. DLS data were analyzed by plotting hydrodynamic radius versus temperature, with aggregation temperatures (T_{agg}) determined as the temperature where the observed hydrodynamic radius (R_h) exceeded twice the baseline radius. T_{onset} values from the MSF experiment were calculated by applying Gaussian fits to melting transitions in the corresponding dBCM data (310–390 nm) using a 1% unfolding threshold. All DSF and MSF results represent the average of three replicate wells, while DLS results are averaged from two replicate wells.

While the expected trend generally holds, particularly among the IgG-type antibodies, notable deviations can occur. Here, we present data for three biologics to illustrate this behavior. It is important to note that these values should be compared with caution, as they represent complex, nonlinear processes occurring over a range of temperatures under non-steady state conditions and are therefore sensitive to the methods used for their acquisition and calculation (defined in the Methods and Materials section).

1. Anti-mouse antibody (IgG): The MSF-derived T_{nr} of 66.2°C occurs shortly after the onset of unfolding ($T_{onset} = 60.8^\circ\text{C}$), with DLS-detected aggregation following at an average T_{agg} of 68.2°C. This behavior aligns with the model described above, indicating that for this antibody even transient unfolding is effectively nonreversible and rapidly leads to aggregation-prone intermediates.
2. Human IgG: The T_{nr} value was the lowest of the three at 63.7°C, 4.4°C above the onset of unfolding ($T_{onset} = 59.3^\circ\text{C}$), indicating that unfolding is nearly synchronous with the onset of irreversible unfolding. However, the DLS T_{agg} of 70.3°C highlights that T_{nr} and T_{agg} do not always occur simultaneously. A protein may form irreversibly unfolded yet soluble species, with aggregation into larger particles occurring more slowly or only at higher temperatures, if at all. This behaviour is taken into account by T_{nr} but not by T_{agg} .
3. HuCAL (Fab): Interestingly, HuCAL exhibits a T_{onset} of 63.8°C, followed by a T_{nr} of 70.2°C, while DLS reports a lower T_{agg} of only 63.8°C. This suggests that aggregation may occur in parallel with or even independently of

unfolding, indicating that the protein becomes colloiddally unstable prior to and without the need for significant conformational destabilization.

Effects of Buffer and pH

As a final example, we examine the DSF and MSF behavior of the model protein lysozyme in buffers at three pH values: 3 (acidic), 7.4 (near physiological/neutral), and 10 (basic). As shown by the dBCM unfolding transitions in Figure 5, lysozyme exhibits comparable conformational stability at pH 3 ($T_m = 72.3^\circ\text{C}$) and pH 7.4 ($T_m = 71.7^\circ\text{C}$), with T_{onset} values differing by only 0.5°C and T_m values by 0.6°C, differences that may be attributable to buffer composition. In contrast, stability is reduced at pH 10, where T_m decreases to 68.4°C, representing a 3.3–3.9°C shift relative to the lower pH conditions. This trend is consistent with a previous report on the thermal stability and nonreversibility of lysozyme at various pH conditions.⁵

These differences are more pronounced in the MSF data. At pH 3, no clear nonreversibility transition is observed, and T_{nr} cannot be determined. Instead, a gradual upward trend is present, suggesting only a minor and largely reversible shift toward a slightly more relaxed (red-shifted) conformational state following thermal perturbation. These results indicate that lysozyme is stable at low pH. At pH 7.4, the onset of irreversible unfolding occurs at 72.9°C, shortly after the midpoint of unfolding (T_m) at 71.7°C. This suggests that early unfolding remains partially reversible over a narrow temperature range before transitioning into a nonreversible, misfolded or aggregated state. At pH 10, however, T_{nr} is observed at 73.2°C, occurring after nearly all of the protein has unfolded.



Table 2: T_{onset} , T_m , and T_{nr} results from an MSF experiment using Lysozyme (pH 3, 7.4, 10) All fitted values represent the mean of three replicate wells.

Lysozyme (pH)	T_{onset} (°C)	T_m (°C)	T_{nr} (°C)
Lysozyme (pH 3)	62.93 ± 0.02	72.29 ± 0.05	No Data
Lysozyme (pH 7.4)	63.42 ± 0.15	71.67 ± 0.04	72.87 ± 0.24
Lysozyme (pH 10)	62.77 ± 0.08	68.41 ± 0.02	73.21 ± 0.13

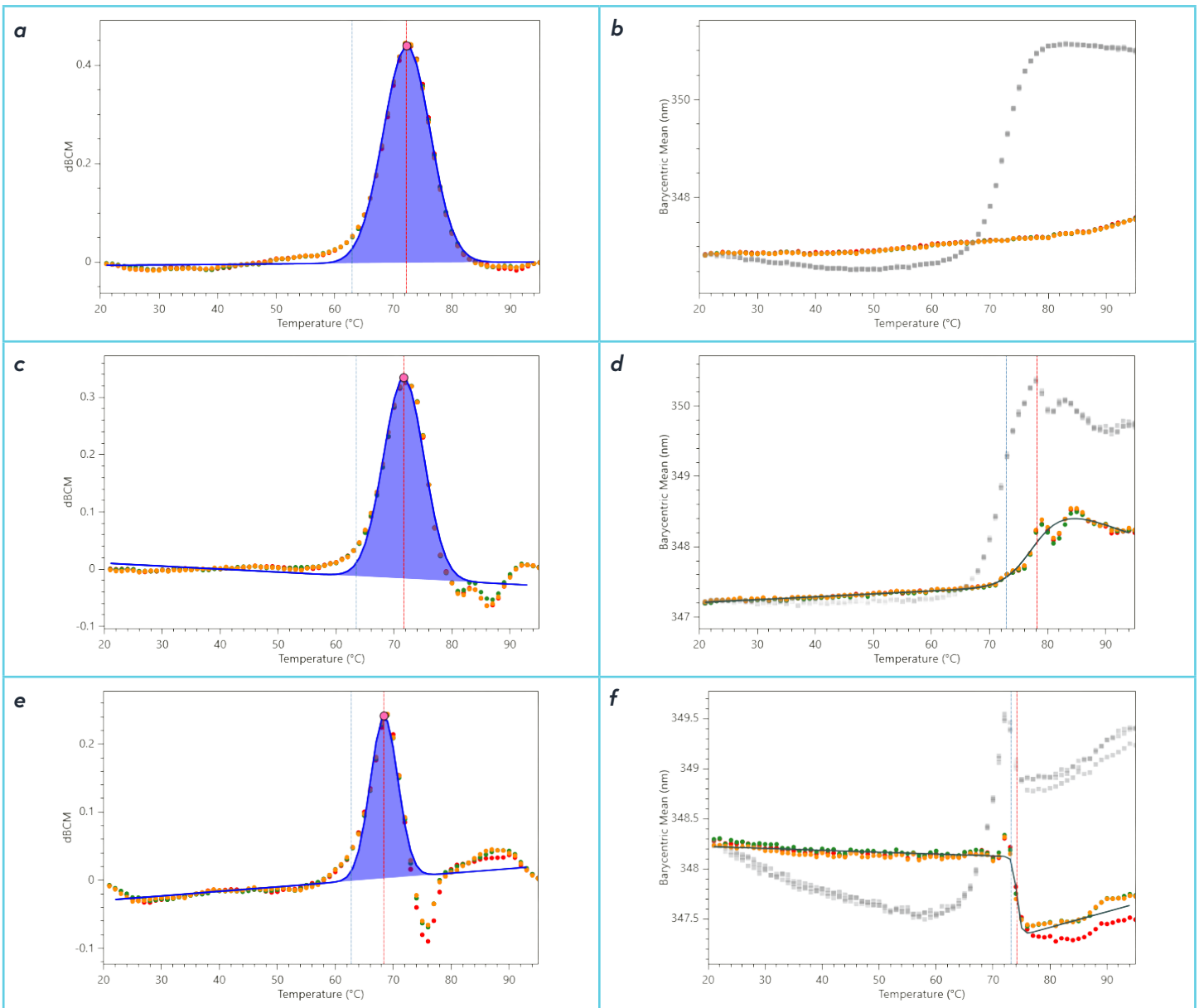


Figure 5: Fitted dBCM plots (a,c,e) and MSF-derived BCM plots (b,d,f) for lysozyme in pH 3 (a,b), pH 7.4 (c,d), and pH 10 (e,f) buffers. Data are plotted in triplicate as dBCM or BCM vs. temperature, respectively. Vertical blue lines indicate T_{onset} (dBCM plots) or T_{nr} (MSF-derived BCM plots), defined as the point at which the fitted curve deviates 1% or 10%, respectively, from the calculated fit baseline. Vertical red lines represent T_m (dBCM plots) or the sigmoidal inflection point of the nonreversibility transition (MSF plots). Gray data points in the MSF plots represent the BCM values for the corresponding melt curve.



Notably, the transition at pH 10 is accompanied by a pronounced blue shift in the BCM data of both the MSF plot, as well as the DSF unfolding curve. Blue shifts in BCM (or ratio-based) DSF signals have been reported to correlate with protein aggregation, unambiguously indicating that this condition promotes not only irreversible unfolding but also concurrent aggregate formation.^{13,14}

More broadly, aggregation propensity is often inversely related to charge density (which is governed by pH) and directly related to the exposure of hydrophobic surfaces during unfolding.¹⁵⁻¹⁷ Lysozyme follows this expected trend: based on its calculated pI (~9.3) and experimentally determined pI (~10.7–11.0), the protein remains highly positively charged at pH 3 and 7.4, but approaches charge neutrality at pH 10.¹⁸ This reduction in electrostatic repulsion likely contributes to the increased aggregation observed following temperature perturbation under basic conditions.

Conclusion

While T_{nr} from MSF and T_{agg} from DLS probe distinct biophysical phenomena—nonreversibility of unfolding (conformational stability) and aggregation onset (colloidal stability), respectively, they are often closely correlated in practice. Importantly, the MSF-derived T_{nr} metric provides additional stability insight not captured by standard DSF or light scattering experiments, enabling earlier detection of irreversible behavior prior to overt aggregation. This additional layer of information is obtained without sacrificing the low cost, minimal sample consumption, and high-throughput workflow characteristic of the SUPR-DSF platform. SUPR-DSF offers a comprehensive solution to protein stability data in a single instrument, including melting temperatures (T_m), onset temperatures (T_{onset}) and nonreversibility of unfolding (T_{nr}).

Materials & Methods

Biological Sample Information

The following commercially available samples were used for the experimental procedures conducted:

- Affinipure® Goat Anti-Mouse IgG (Jackson ImmunoResearch, 115-005-146)
- IgG from Human Serum (InvivoGen, 12577)
- HuCAL Fab-FH Negative Control (BioRad, HCA045)
- Lysozyme (BioShop, LYS702)

DSF & MSF Methods

Sample Preparation

1. Samples: All samples were diluted in PBS (pH 7.4) to a final concentration of 0.9 mg/mL. For MSF experiments with lysozyme at varying pH, samples were prepared in 10 mM glycine-HCl (pH 3) and 20 mM CAPS (pH 10), with no additional salt added to either buffer.
2. Plate Loading & Replicates: All samples (10 μ L aliquots per well) were pipetted into a standard black 384-well PCR microplate (FrameStar™ 384-Well Skirted PCR Plate; Azenta Life Sciences, 4ti-0386), using triplicate wells per condition. Two identical plates were prepared for DSF and MSF experiments, respectively.
3. Sealing: The plate was briefly centrifuged and then sealed with an optically clear, pressure-activated adhesive film (qPCR Adhesive Seal; Azenta Life Sciences, 4ti-0560) to prevent sample evaporation and concentration changes during the thermal ramp.
4. Data Acquisition: The SUPR-DSF instrument was configured for separate DSF and MSF experiment types using the parameters listed below.

Differential Scanning Fluorimetry (DSF)

Thermal unfolding (T_{onset} & T_m) was directly measured in a traditional DSF experiment using a linear thermal temperature gradient.

- Temperature range: 20°C to 105°C
- Ramp rate: 1°C per minute
- Excitation: 280 nm
- 154 total spectra were obtained from each sample (scan interval = 0.5°C)
- Integration time: 25 ms
- Detection: Full spectrum fluorescence emission (310–420 nm)
- Total experiment time: 75 minutes

SUPR-Suite software (v2.1.4.0) was used for data acquisition and analysis. Spectral data were processed using the Barycentric Mean (BCM) method over 310–390 nm, and melting temperatures (T_m) were determined from the corresponding first-derivative (dBCM; Gaussian) fits using the SUPR-Suite's proprietary autofitting algorithm.



Modulated Scanning Fluorimetry (MSF)

Nonreversibility of thermal unfolding (T_{nr}) was measured in an MSF experiment using a temperature cycling methodology. Thermal unfolding (T_{onset} & T_m) values were also obtained from this experiment and are tabulated below for comparison.

- Start temperature: 20°C
- End temperature: 95°C
- Temperature increment: 1°C
- Ramp rate: 12°C per minute
- Incubation time: 1 minute
- Recovery period: 5 minutes
- Excitation: 280 nm
- Integration time: 25 ms
- Detection: Full spectrum fluorescence emission (310-420 nm)
- Total experiment time: 18 hours

SUPR-Suite software (v2.1.4.0) was used for data acquisition and analysis. Spectral data were processed using the Barycentric Mean (BCM) method over 310–390 nm.

- Melting temperatures (T_{onset} & T_m) were determined by fitting the first-derivative (dBCM) data with Gaussian fits using the SUPR-Suite's proprietary autofitting algorithm.
- Non-reversibility temperatures (T_{nr}) were calculated from the BCM data via the SUPR-Suite's proprietary autofitting algorithm with T_{nr} defined as the temperature at which 10% of the protein shows non-reversible behavior, as determined from a sigmoidal fit to the recovery-period fluorescence signal. For calculating DSF results, fluorescence report points were taken during the incubation periods of each cycle, and for calculating MSF results, fluorescence report points were taken during the 20°C recovery periods between cycles.

Dynamic Light Scattering (DLS) Methods

Sample Preparation

1. Samples: All samples were diluted into PBS (pH 7.4) at 0.9 mg/mL final concentration.
2. Plate Loading & Replicates: All samples (20 μ L aliquots per well) were pipetted into a black 384-well PCR microplate with clear bottom (Aurora® 384 Round; Wyatt Technology LLC, P8806-38403), using duplicate wells per condition.
3. Sealing: The plate was briefly centrifuged and then sealed with 10 μ L paraffin oil (Sigma, 76235) to prevent

sample evaporation and concentration changes during the thermal ramp.

4. Data Acquisition: The DynaPro Plate Reader III Dynamic & Static Light Scattering (DLS & SLS) instrument was configured for temperature ramping using the parameters listed below.

Experimental Conditions

Thermal unfolding (T_{agg}) was directly measured in a DLS experiment using a linear thermal temperature gradient.

- Temperature range: 25°C to 85°C
- Ramp rate: 0.387097°C per minute
- DLS acquisition time: 5 s
- DLS Acquisitions per measurement: 3
- Total experiment time: 198 minutes

The DYNAMICS™ software suite was used for data acquisition. Data were analyzed by plotting hydrodynamic radius (R_h) as a function of temperature, and aggregation temperatures (T_{agg}) were determined as follows: the R_h trace was first smoothed using a median filter to remove single-point spikes, followed by a moving average to reduce noise. The baseline was defined as the lowest-variance 10-point window within the first half of the smoothed trace. T_{agg} was then assigned as the first temperature at which five consecutive data points exceeded either the baseline by 10 nm or twice the baseline value, whichever was greater. Results are shown in Figure 6.

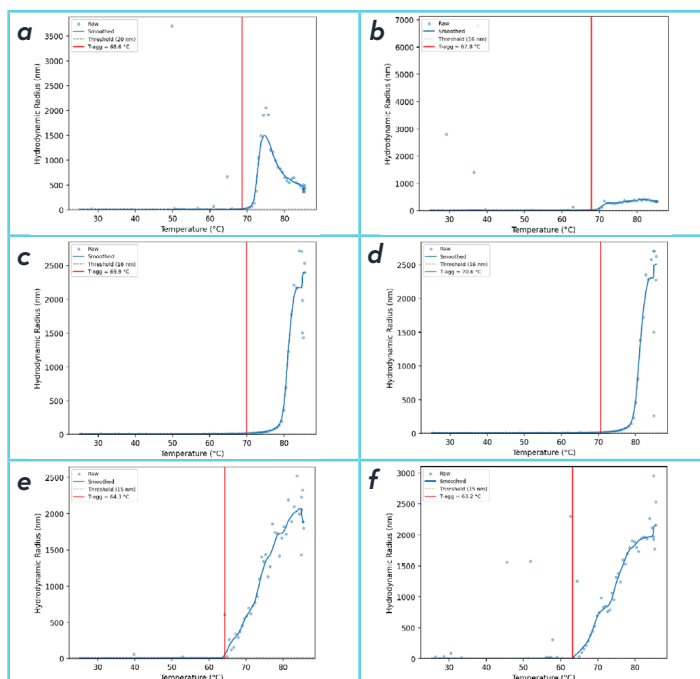


Figure 6: Duplicate DLS data following acquisition, processing, and fitting for a,b) Anti-mouse c,d) Human IgG and e,f) HuCAL



References

1. Jain, T.; Sun, T.; Durand, S.; Hall, A.; Houston, N. R.; Nett, J. H.; Sharkey, B.; Bobrowicz, B.; Caffry, I.; Yu, Y.; Cao, Y.; Lynaugh, H.; Brown, M.; Baruah, H.; Gray, L. T.; Krauland, E. M.; Xu, Y.; Vásquez, M.; Wittrup, K. D. Biophysical Properties of the Clinical-Stage Antibody Landscape. *Proc. Natl. Acad. Sci. U. S. A.* 2017, 114 (5), 944–949. <https://doi.org/10.1073/pnas.1616408114>
2. Gentiluomo, L.; Svilenov, H. L.; Augustijn, D.; El Bialy, I.; Greco, M. L.; Kulakova, A.; Indrakumar, S.; Mahapatra, S.; Morales, M. M.; Pohl, C.; Roche, A.; Tosstorff, A.; Curtis, R.; Derrick, J. P.; Nørgaard, A.; Khan, T. A.; Peters, G. H. J.; Pluen, A.; Rinnan, Å.; Streicher, W. W.; van der Walle, C. F.; Uddin, S.; Winter, G.; Roessner, D.; Harris, P.; Frieß, W. Advancing Therapeutic Protein Discovery and Development through Comprehensive Computational and Biophysical Characterization. *Mol. Pharm.* 2020, 17 (2), 426–440. <https://doi.org/10.1021/acs.molpharmaceut.9b00852>
3. Cohrs, M.; Davy, A.; Van Ackere, M.; De Smedt, S.; Braeckmans, K.; Epe, M.; Svilenov, H. L. Intrinsic Differential Scanning Fluorimetry for Protein Stability Assessment in Microwell Plates. *Mol. Pharmaceutics* 2025, 22 (3), 1697–1706. <https://doi.org/10.1021/acs.molpharmaceut.4c01496>
4. Roberts, C. J. Non-Native Protein Aggregation Kinetics. *Biotechnol. Bioeng.* 2007, 98 (5), 927–938. <https://doi.org/10.1002/bit.21627>
5. Svilenov, H. L.; Menzen, T.; Richter, K.; Winter, G. Modulated Scanning Fluorimetry Can Quickly Assess Thermal Protein Unfolding Reversibility in Microvolume Samples. *Mol. Pharmaceutics* 2020, 17 (7), 2638–2647. <https://doi.org/10.1021/acs.molpharmaceut.0c00330>
6. Berner, C.; Menzen, T.; Winter, G.; Svilenov, H. L. Combining Unfolding Reversibility Studies and Molecular Dynamics Simulations to Select Aggregation-Resistant Antibodies. *Mol. Pharmaceutics* 2021, 18 (6), 2242–2253. <https://doi.org/10.1021/acs.molpharmaceut.1c00017>
7. Pérez, J. M. J.; Renisio, J. G.; Prompers, J. J.; Van Platerink, C. J.; Cambillau, C.; Darbon, H.; Frenken, L. G. J. Thermal Unfolding of a Llama Antibody Fragment: A Two-State Reversible Process. *Biochemistry* 2001, 40, 74–83. <https://doi.org/10.1021/bi0009082>
8. Jespers, L.; Schon, O.; Famm, K.; Winter, G. Aggregation-Resistant Domain Antibodies Selected on Phage by Heat Denaturation. *Nat. Biotechnol.* 2004, 22, 1161–1165. <https://doi.org/10.1038/nbt1000>
9. Famm, K.; Hansen, L.; Christ, D.; Winter, G. Thermodynamically Stable Aggregation-Resistant Antibody Domains through Directed Evolution. *J. Mol. Biol.* 2008, 376, 926–931. <https://doi.org/10.1016/j.jmb.2007.10.075>
10. Arbabi-Ghahroudi, M.; To, R.; Gaudette, N.; Hiram, T.; Ding, W.; MacKenzie, R.; Tanha, J. Aggregation-Resistant VHs Selected by in Vitro Evolution Tend to Have Disulfide-Bonded Loops and Acidic Isoelectric Points. *Protein Eng., Des. Sel.* 2008, 22, 59–66. <https://doi.org/10.1093/protein/gzn071>
11. Kim, D. Y.; To, R.; Kandalaf, H.; Ding, W.; Van Faassen, H.; Luo, Y.; Schrag, J. D.; St-Amant, N.; Hefford, M.; Hiram, T.; et al. Antibody Light Chain Variable Domains and Their Biophysically Improved Versions for Human Immunotherapy. *mAbs* 2014, 6, 219–235. <https://doi.org/10.4161/mabs.26844>
12. Andersen, C. B.; Manno, M.; Rischel, C.; Thórolfsson, M.; Martorana, V. Aggregation of a Multidomain Protein: A Coagulation Mechanism Governs Aggregation of a Model IgG1 Antibody under Weak Thermal Stress. *Protein Sci.* 2010, 19(2), 279–290. <https://doi.org/10.1002/pro.309>
13. Kim, S. H.; Yoo, H. J.; Park, E. J.; Na, D. H. Nano Differential Scanning Fluorimetry-Based Thermal Stability Screening and Optimal Buffer Selection for Immunoglobulin G. *Pharmaceuticals* 2022, 15 (1), 29. <https://doi.org/10.3390/ph15010029>
14. Xin, L.; Prorok, M.; Zhang, Z.; Barboza, G.; More, R.; Bonfiglio, M.; Cheng, L.; Robbie, K.; Ren, S.; Li, Y. Rapid Development of High Concentration Protein Formulation Driven by High-Throughput Technologies. *Pharm. Res.* 2025, 42 (1), 151–171. <https://doi.org/10.1007/s11095-024-03801-3>
15. Arakawa, T.; Timasheff, S. N. The Stabilization of Proteins by Osmolytes. *Biophys. J.* 1985, 47 (3), 411–414. [https://doi.org/10.1016/S0006-3495\(85\)83932-1](https://doi.org/10.1016/S0006-3495(85)83932-1)
16. Chi, E. Y.; Krishnan, S.; Randolph, T. W.; Carpenter, J. F. Physical Stability of Proteins in Aqueous Solution: Mechanism and Driving Forces in Nonnative Protein Aggregation. *Pharm. Res.* 2003, 20 (9), 1325–1336. <https://doi.org/10.1023/A:1025771421906>
17. Wang, W. Protein Aggregation and Its Inhibition in Biopharmaceutics. *Int. J. Pharm.* 2005, 289 (1–2), 1–30. <https://doi.org/10.1016/j.ijpharm.2004.11.014>
18. Canfield, R. E. The Amino Acid Sequence of Egg White Lysozyme. *J. Biol. Chem.* 1963, 238 (8), 2698–2707. [https://doi.org/10.1016/S0021-9258\(18\)67888-3](https://doi.org/10.1016/S0021-9258(18)67888-3)

